

TRANSIENT THERMOELASTIC ANALYSIS IN THIN
ANNULAR DISC WITH RADIATION TYPE
BOUNDARIES CONDITIONS

Vinod Varghese¹, Namdeo W. Khobragade² §

^{1,2}Department of Mathematics

MJP Educational Campus

Nagpur University

Nagpur, 440 010, INDIA

²e-mail: khobragade_nw@rediffmail.com

Abstract: By the theory of integral transformation technique, the thermoelastic problem of a thin annular disc with boundary conditions of radiation type is theoretically treated on the edge of the curved surface occupying the region under consideration. Temperature distribution, displacement and stress functions of a thin annular disc with a known partially distributed heat supply along the curved surface are evaluated. Numerical estimates for heating and cooling processes subjected to partially distributed heat supply on the boundary $z = h$ have been obtained and depicted graphically.

AMS Subject Classification: 35A25, 74M99, 74K20

Key Words: transient response, annular disc, temperature distribution, thermal stress, integral transform

1. Introduction

Nowacki [5] has determined steady-state thermal stresses in a circular plate subjected to an axisymmetric temperature distribution on the upper face with zero temperature on the lower face and circular edge. Roy Choudhuri [6] has succeeded in determining the quasi-static thermal stresses in a circular plate subjected to transient temperature along the circumference of circular upper face with lower face is at zero temperature and the fixed circular edge thermally insulated. Wankhede [8] has determined the quasi-static thermal stresses

Received: June 7, 2007

© 2007, Academic Publications Ltd.

§Correspondence author

in circular plate subjected to arbitrary initial temperature on the upper face with lower face at zero temperature. Noda et al [1] have considered a circular plate and discussed the transient thermoelastic-plastic bending problem, making use of the strain increment theorem. Khobragade et al [3] have studied the partially distributed heat supply of a thin circular plate applying finite Hankel and Fourier transform using Dirichlet type of boundary conditions. Varghese et al [2] have studied the inverse thermoelastic problem of a thin annular plate using Integral transform techniques. In the present paper, an attempt is made to study the theoretical solution for a thermoelastic problem to determine the temperature distribution, displacement and stress functions of a thin annular disc with boundary conditions of radiation type and subjected to known partially distributed heat supply $-(Q_0/\lambda)f(r, t)$ occupying the space $D = \{(x, y, z) \in R^3 : a \leq (x^2 + y^2)^{1/2} \leq b, 0 \leq z \leq h\}$, where $r = (x^2 + y^2)^{1/2}$. A transform defined by Zgrablich et al [4] is used for investigation which is a generalization of Hankel's double radiation finite transform and used to treat the problem with radiation type boundaries conditions. The significance of aforementioned transform over previous used or published integral transform techniques can be seen while obtaining the temperature or displacement of any height, with boundary conditions of radiation type on the outside and inside surfaces, with independent radiation constant. A brief note contains relevant results of the transform, although elementary, are not easily found in textbooks provided in Section 2.

2. The Transformation and its Essential Property (see [4])

The finite integral transform of $f(r)$ is defined as

$$\bar{f}_p(n) = \int_a^b r f(r) S_p(\alpha, \beta, \mu_n r) dr, \quad (2.1)$$

with $\alpha_1, \alpha_2, \beta_1$ and β_2 are the constants involved in the boundary conditions $\alpha_1 f(r) + \alpha_2 f'(r)|_{r=a} = 0$ and $\beta_1 f(r) + \beta_2 f'(r)|_{r=b} = 0$ for the differential equation $f''(r) + (1/r)f'(r) - (p^2/r^2)f(r) = 0$, $\bar{f}_p(n)$ is the transform of $f(r)$ with respect to nucleus $S_p(\alpha, \beta, \mu_n r)$ and weight function r . The eigenvalues μ_n are the positive roots of the frequency of characteristic equation $J_p(\bar{k}_1, \mu a) Y_p(\bar{k}_2, \mu b) - J_p(\bar{k}_2, \mu b) Y_p(\bar{k}_1, \mu a) = 0$, with $\bar{k}_1 = \alpha_2/\alpha_1$, $\bar{k}_2 = \beta_2/\beta_1$ as radiation constants. The inversion of equation (2.1) is given by

$$f(r) = \sum_{n=1}^{\infty} \frac{\bar{f}_p(n) S_p(\alpha, \beta, \mu_n r)}{\int_0^t [r S_p(\alpha, \beta, \mu_n r)]^2 dr}, \quad (2.2)$$

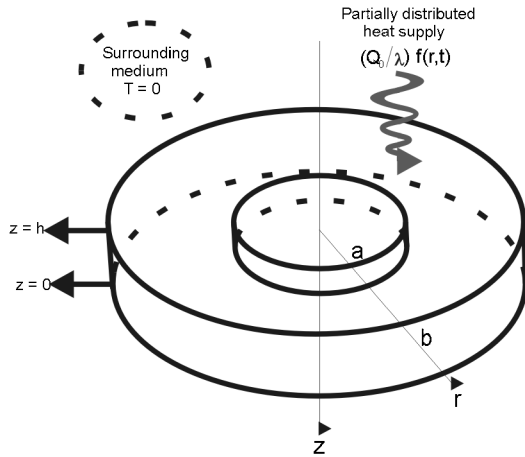


Figure 1: The configuration of thin annular disc

where kernel function $S_p(\alpha, \beta, \mu_n r)$ can be defined as

$$S_p(\alpha, \beta, \mu_n r) = J_p(\mu_n r)[Y_p(\alpha, \mu_n a) + Y_p(\beta, \mu_n b)] + Y_p(\mu_n r)[J_p(\alpha, \mu_n a) + J_p(\beta, \mu_n b)], \quad (2.3)$$

in which $J_p(\mu_n r)$ and $Y_p(\mu_n r)$ are Bessel function of first and second kind of order p respectively.

3. Formulation of the Problem: Governing Equation

Consider a thin annular disc of thickness h occupying the space D . The initial temperature of the disc is same as the temperature of the surrounding medium, which is kept constant for the time $0 \leq t \leq t_0$, the disc is subjected to a partially distributed heat supply from the upper surface. After that, the heat supply is removed and disc is cooled by the surrounding medium. For small thickness of disc in a plane state of stress, the displacement equations of thermoelasticity [6, 3] can be defined as

$$\phi_{i,kk} + \frac{1 + \nu}{1 - \nu} e_{,i} = 2 \frac{1 + \nu}{1 - \nu} \alpha_t T_{,i}, \quad (3.1)$$

$$e = \phi_{kk}, \quad \text{for } i, k = 1, 2, \quad (3.2)$$

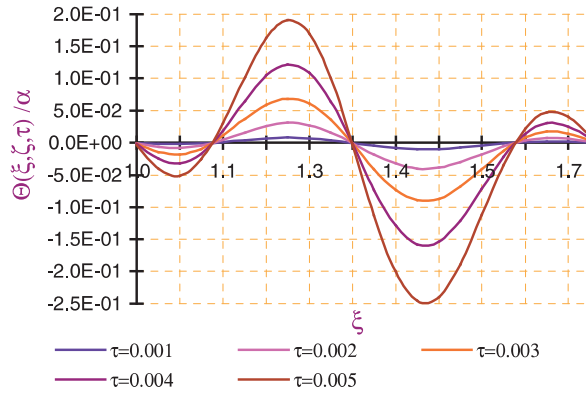


Figure 2: Distribution of the dimensionless temperature Θ versus dimensionless radius ξ for $\zeta = 0.02$ and different values of dimensionless time τ in heating processes

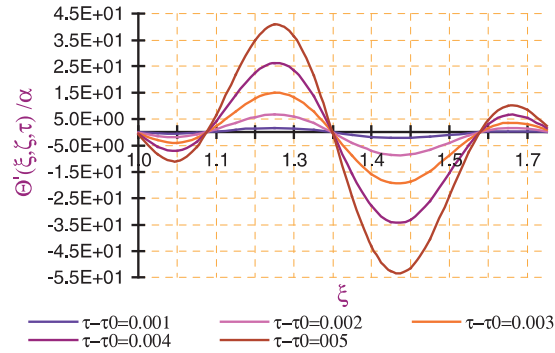


Figure 3: Distribution of the dimensionless temperature Θ versus dimensionless radius ξ for $\zeta = 0.02$ and different values of dimensionless time τ in cooling processes

Introducing $\phi_i = \phi_{,i}$ ($i = 1, 2$), we have

$$\nabla_1^2 \phi = (1 + \nu) a_t T, \tag{3.3}$$

where

$$\nabla_1^2 \phi = \frac{\partial^2}{\partial k_1^2} + \frac{\partial^2}{\partial k_2^2}. \tag{3.4}$$

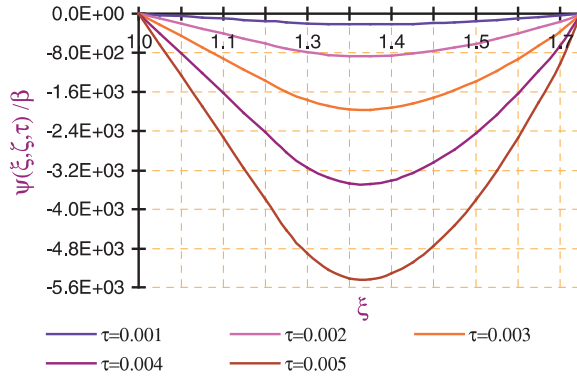


Figure 4: Distribution of the dimensionless displacement function ψ versus dimensionless radius ξ for $\zeta = 0.02$ and different values of dimensionless time τ

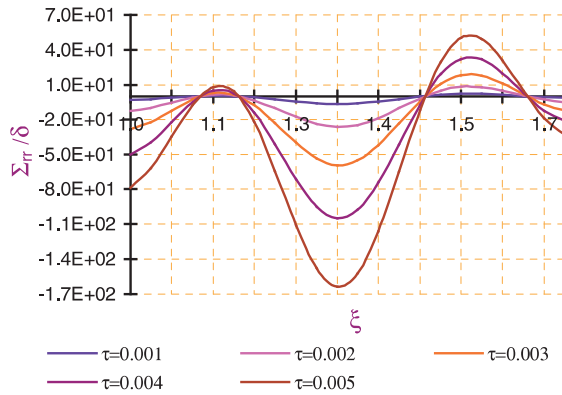


Figure 5: Distribution of the dimensionless radial stress Σ_{rr} versus dimensionless radius ξ for $\zeta = 0.02$ and different values of dimensionless time τ

The stress σ_{ij} is given by

$$\sigma_{ij} = 2\mu(\phi_{,ij} - \delta_{,ij}\phi_{,kk}), \quad \text{for } i, j, k = 1, 2. \tag{3.5}$$

The differential equation governing the displacement function $\phi(r, z, t)$, for the

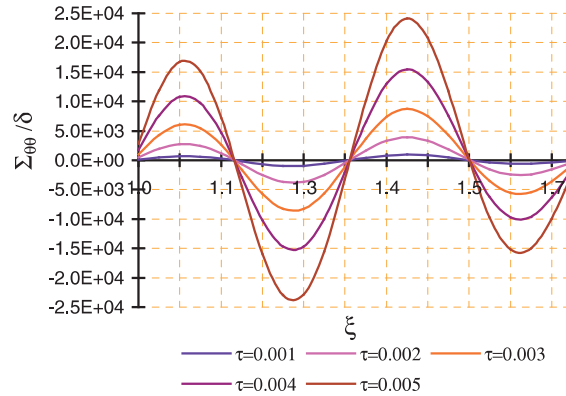


Figure 6: Distribution of the dimensionless axial stress $\Sigma_{\theta\theta}$ versus dimensionless radius ξ for $\zeta = 0.02$ and different values of dimensionless time τ

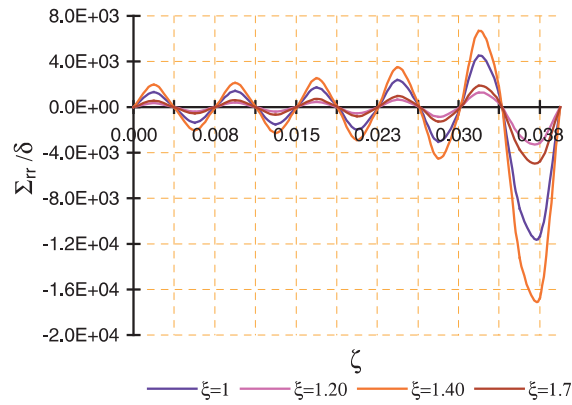


Figure 7: Distribution of the dimensionless radial stress Σ_{rr} versus dimensionless thickness ζ for $\tau = 0.02$ and different values of dimensionless radius ξ

heating and cooling process is given as

$$\frac{\partial^2 \phi}{\partial r^2} + \frac{1}{r} \frac{\partial \phi}{\partial r} = (1 + \nu)\theta, \tag{3.6}$$

$$\text{with } \phi(r, z, t) = 0 \text{ at } r = a \text{ for all time } t, \tag{3.7}$$

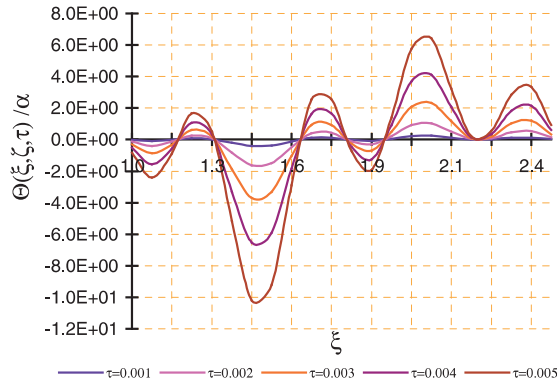


Figure 8: Distribution of the dimensionless temperature Θ versus dimensionless radius ξ for $\zeta = 0.02$ and different values of dimensionless time τ in heating processes with $\eta = 0.02$

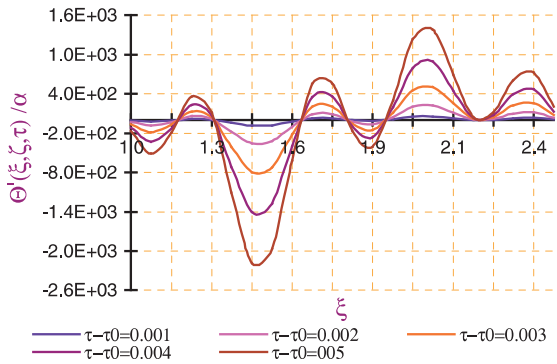


Figure 9: Distribution of the dimensionless temperature Θ versus dimensionless radius ξ for $\zeta = 0.02$ and different values of dimensionless time τ in cooling processes with $\eta = 0.02$

where $\phi(r, z, t)$ is the displacement component, δ_{ij} is the well-known Kronecker symbol, e is the dilatation, ν and a_t are the Poisson's ratio and the linear coefficient of thermal expansion of the material of the disc respectively and $T(r, z, t)$ is the heating temperature of the disc at time t satisfying the differential equa-

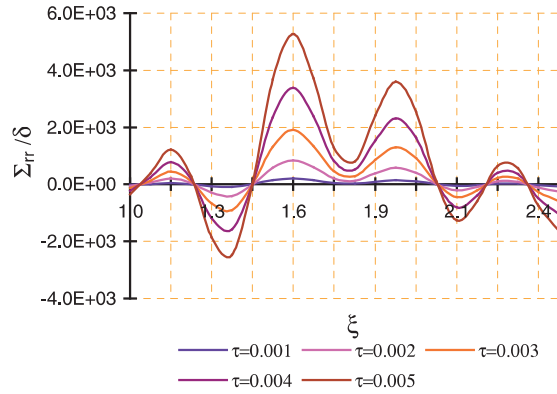


Figure 10: Distribution of the dimensionless radial stress Σ_{rr} versus dimensionless radius ξ for $\zeta = 0.02$ and different values of dimensionless time τ with $\eta = 0.02$

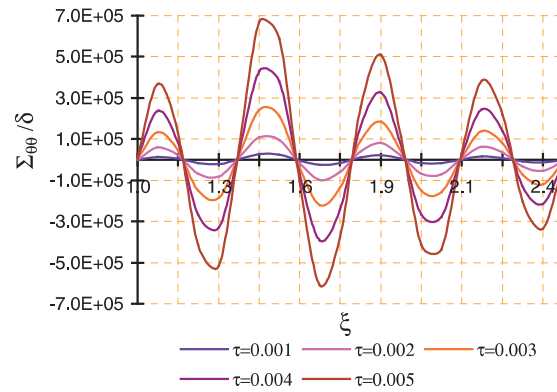


Figure 11: Distribution of the dimensionless axial stress $\Sigma_{\theta\theta}$ versus dimensionless radius ξ for $\zeta = 0.02$ and different values of dimensionless time τ with $\eta = 0.02$

tion

$$\frac{1}{r} \frac{\partial}{\partial r} \left(r \frac{\partial T}{\partial r} \right) + \frac{\partial^2 T}{\partial z^2} = \frac{1}{\kappa} \frac{\partial T}{\partial t} \tag{3.8}$$

where $\kappa = K/c\rho$ is the thermal diffusivity of the material of the disc, K is the conductivity of the medium, c is its specific heat and ρ is its calorific ca-

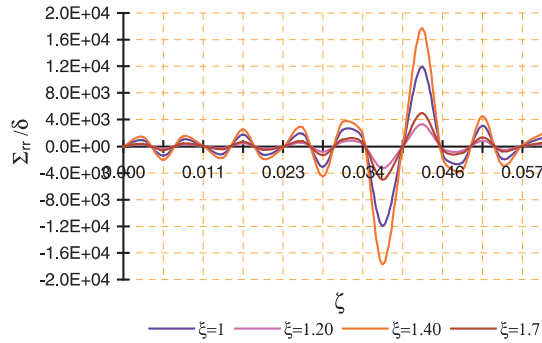


Figure 12: Distribution of the dimensionless radial stress Σ_{rr} versus dimensionless thickness ζ ($=0.60$) for $\tau = 0.02$ and different values of dimensionless radius ξ

capacity (which is assumed to be constant), subject to the initial and boundary conditions

$$M_t(T, 1, 0, 0) = 0 \text{ for all } 0 \leq r \leq a \text{ and } 0 \leq z \leq h, \tag{3.9}$$

$$M_r(T, 1, \bar{k}_1, a) = F_1(z, t), M_r(T, 1, \bar{k}_2, b) = F_2(z, t), \tag{3.10}$$

for all $0 \leq z \leq h$ and $t > 0$,

$$M_z(T, 1, 0, 0) = g(r, t), M_z(T, 1, 0, h) = -(Q_0/\lambda)f(r, t), \tag{3.11}$$

for all $a \leq r \leq b$ and $t > 0$.

On the other hand, for the cooling process, the temperature change $T'(r, z, t)$ satisfies the equation

$$\frac{1}{r} \frac{\partial}{\partial r} \left(r \frac{\partial T'}{\partial r} \right) + \frac{\partial^2 T'}{\partial z^2} = \frac{1}{\kappa} \frac{\partial T'}{\partial t}, \tag{3.12}$$

with the initial and boundary conditions

$$M_t(T, 1, 0, 0) = M_t(T', 1, 0, t_0), \text{ for all } 0 \leq r \leq a \text{ and } 0 \leq z \leq h, \tag{3.13}$$

$$M_r(T', 1, \bar{k}_1, a) = 0, M_r(T', 1, \bar{k}_2, b) = 0, \text{ for all } 0 \leq z \leq h \text{ and } t > t_0, \tag{3.14}$$

$$M_z(T', 1, 0, 0) = 0, M_z(T', 1, 0, h) = 0, \text{ for all } a \leq r \leq b \text{ and } t > t_0. \tag{3.15}$$

being:

$$M_{\vartheta}(g, \bar{k}, \bar{\bar{k}}, \tilde{s}) = (\bar{k}g + \bar{\bar{k}}\hat{g})_{\vartheta=\tilde{s}}, \tag{3.16}$$

where the prime ($\hat{}$) denotes differentiation with respect to ϑ and the radiation constants are postulated as \bar{k} and $\bar{\bar{k}}$ on the curved surfaces of the disc respectively. The functions $g(r, t)$, $F_1(z, t)$ and $F_2(z, t)$ are known constants and they

are set to be zero here as in other literatures Marchi et al [4] and Khobragade [2] so as to obtain considerable mathematical simplicities.

The stress distribution components σ_{rr} and $\sigma_{\theta\theta}$ of the disc for the heating and the cooling process are given by

$$\sigma_{rr} = -2\mu \frac{1}{r} \frac{\partial \phi}{\partial r}, \quad (3.17)$$

$$\sigma_{\theta\theta} = -2\mu \frac{1}{r} \frac{\partial^2 \phi}{\partial r^2}, \quad (3.18)$$

where μ is the Lamé's constants, while each of the stress functions, σ_{rz} , σ_{zz} and $\sigma_{\theta z}$ are zero within the plate in the plane state of stress. Thus, the equations (3.6) to (3.18) constitute the mathematical formulation of the problem under consideration.

4. Solution of the Problem

4.1. Determination of the Temperatures $T(r, z, t)$ and $T'(r, z, t)$

Applying transform defined in equation (2.1) to the equations (3.8), (3.9) and (3.11) over the variable r having $p = 0$ with responds to the boundary conditions of type (3.10) and taking the Laplace transform [7], one obtains

$$\bar{T}^* = - \left(\frac{Q_0}{\lambda} \right) \bar{f}(n, s) \left(\frac{\sinh(qz)}{\sinh(\xi z)} \right) \quad (4.1)$$

where $q^2 = \mu_n^2 + (s/\kappa)$ and the constants are obtained with the use of boundary conditions (3.9)-(3.10). Applying the inversion theorems of transform (2.2) and inverse Laplace transform by means of complex contour integration and the residue theorem, one obtains the expression of the temperature distribution $T(r, z, t)$ for heating processes as

$$T(r, z, t) = \left(\frac{2\kappa Q_0}{\lambda h} \right) \sum_{n=1}^{\infty} \frac{1}{C_n} \sum_{l=0}^{\infty} \varphi_{nl} S_0(\bar{k}_1, \bar{k}_2, \mu_n r). \quad (4.2)$$

On the other hand, for the cooling process, applying transform defined in equation (2.1) and Fourier sine transform [7] to the equations (3.12) to (3.15) and then using their inversions, one obtains the expression of the temperature distribution $T'(r, z, t)$ as

$$T'(r, z, t) = \left(\frac{4\kappa Q_0}{\lambda h^2} \right) \sum_{n=1}^{\infty} \frac{1}{C_n} \sum_{m=1}^{\infty} \sin \left(\frac{m\pi z}{h} \right) \sum_{l=0}^{\infty} \psi_{nl} S_0(\bar{k}_1, \bar{k}_2, \mu_n r), \quad (4.3)$$

where

$$\begin{aligned} \varphi_{nl} &= \frac{\lambda_l \sin(\lambda_l z)}{\cos(\lambda_l h)} \int_0^t \bar{f}(n, t') \exp[-\kappa(\mu_n^2 + \lambda_l^2)(t - t')] dt', \\ \psi_{nl} &= \frac{\lambda_l \sin(\lambda_l z)}{\cos(\lambda_l h)} \int_0^t \bar{f}(n, t') \exp[-\kappa(\mu_n^2 + p^2)(t - t_0)] dt' \end{aligned}$$

in which n is the transformation parameter defined in Section 2, m is the Fourier sine transform parameter, $\lambda_l = l\pi/h$ and $p = m\pi/h$.

4.2. Determination of Displacement Function

Substituting the value of $T(r, z, t)$ from equation (4.2) in equation (3.6) and using the well known standard result

$$\left(\frac{\partial^2}{\partial r^2} + \frac{1}{r} \frac{\partial}{\partial r} \right) J_0(\xi_n r) = -\xi_n^2 J_0(\xi_n r), \tag{4.4}$$

one obtains the thermoelastic displacement function as

$$\phi(r, z, t) = -(1 + \nu) a_t \left(\frac{2\kappa Q_0}{\lambda h} \right) \sum_{n=1}^{\infty} \frac{1}{C_n} \sum_{l=0}^{\infty} \varphi_{nl} S_0(\bar{k}_1, \bar{k}_2, \mu_n r). \tag{4.5}$$

4.3. Determination of Stress Function

Substituting the value of equation (4.5) in equations (3.17) and (3.18) and using the well known standard results

$$\frac{\partial}{\partial r} (J_0(\xi_n r)) = -\xi_n J_1(\xi_n r) \tag{4.6}$$

and

$$\frac{\partial^2}{\partial r^2} (J_0(\xi_n r)) = -\xi_n^2 \left(J_0(\xi_n r) - \frac{J_1(\xi_n r)}{\xi_n r} \right) \tag{4.7}$$

one obtains the expressions of the stress functions as

$$\sigma_{rr} = 2\mu(1 + \nu) a_t \left(\frac{2\kappa Q_0}{\lambda h} \right) \sum_{n=1}^{\infty} \frac{1}{C_n \mu_n} \sum_{l=0}^{\infty} \varphi_{nl} S'_0(\bar{k}_1, \bar{k}_2, \mu_n r), \tag{4.8}$$

$$\sigma_{\theta\theta} = 2\mu(1 + \nu) a_t \left(\frac{2\kappa Q_0}{\lambda h} \right) \sum_{n=1}^{\infty} \frac{1}{C_n} \sum_{l=0}^{\infty} \varphi_{nl} S''_0(\bar{k}_1, \bar{k}_2, \mu_n r). \tag{4.9}$$

5. Special Case

Set

$$f(r, t) = (e^t - 1)\delta(r - r_0)(e^h - 1). \quad (5.1)$$

Applying finite transform stated in (2.1) to the equation (5.1) one obtains

$$\bar{f}(n, t) = (e^t - 1)r_0 S_0(\bar{k}_1, \bar{k}_2, \mu_n r_0)(e^h - 1). \quad (5.2)$$

Substituting the value of (5.2) in the equations (4.2), (4.3), (4.5), (4.8) and (4.9) one obtains

$$T(r, z, t) = \left(\frac{2\kappa Q_0}{\lambda h}\right) \sum_{n=1}^{\infty} \frac{1}{C_n} \sum_{l=0}^{\infty} r_0 \Phi_{nl} S_0(\bar{k}_1, \bar{k}_2, \mu_n r_0) S_0(\bar{k}_1, \bar{k}_2, \mu_n r), \quad (5.3)$$

$$\begin{aligned} T'(r, z, t) &= \left(\frac{4\kappa Q_0}{\lambda h^2}\right) \sum_{n=1}^{\infty} \frac{1}{C_n} \sum_{m=1}^{\infty} \sin\left(\frac{m\pi z}{h}\right) \\ &\quad \times \sum_{l=0}^{\infty} r_0 \Omega_{nl} S_0(\bar{k}_1, \bar{k}_2, \mu_n r_0) S_0(\bar{k}_1, \bar{k}_2, \mu_n r), \end{aligned} \quad (5.4)$$

$$\begin{aligned} \phi(r, z, t) &= -(1 + \nu) a_t \left(\frac{2\kappa Q_0}{\lambda h}\right) \sum_{n=1}^{\infty} \frac{1}{C_n} \\ &\quad \times \sum_{l=0}^{\infty} r_0 \Phi_{nl} S_0(\bar{k}_1, \bar{k}_2, \mu_n r_0) S_0(\bar{k}_1, \bar{k}_2, \mu_n r), \end{aligned} \quad (5.5)$$

$$\begin{aligned} \sigma_{rr} &= 2\mu(1 + \nu) a_t \left(\frac{2\kappa Q_0}{\lambda h}\right) \sum_{n=1}^{\infty} \frac{1}{C_n \mu_n} \\ &\quad \times \sum_{l=0}^{\infty} r_0 \Phi_{nl} S_0(\bar{k}_1, \bar{k}_2, \mu_n r_0) \varphi_{nl} S'_0(\bar{k}_1, \bar{k}_2, \mu_n r), \end{aligned} \quad (5.6)$$

$$\begin{aligned} \sigma_{\theta\theta} &= 2\mu(1 + \nu) a_t \left(\frac{2\kappa Q_0}{\lambda h}\right) \sum_{n=1}^{\infty} \frac{1}{C_n} \\ &\quad \times \sum_{l=0}^{\infty} r_0 \Phi_{nl} S_0(\bar{k}_1, \bar{k}_2, \mu_n r_0) S''_0(\bar{k}_1, \bar{k}_2, \mu_n r), \end{aligned} \quad (5.7)$$

where

$$\Phi_{nl} = \frac{\lambda_l \sin(\lambda_l z)}{\cos(\lambda_l h)} \int_0^t (e^{t'} - 1)(e^h - 1) \exp[-\kappa(\mu_n^2 + \lambda_l^2)(t - t')] dt',$$

$$\Omega_{nl} = \frac{\lambda_l \sin(\lambda_l z)}{\cos(\lambda_l h)} \int_0^t (e^{t'} - 1)(e^h - 1) \exp[-\kappa(\mu_n^2 + p^2)(t - t_0)] dt'.$$

6. Convergence of the Series Solution

In order for the solution to be meaningful the series expressed in equations (4.2) and (4.2) should converge for all $a \leq r \leq b$ and $0 \leq z \leq h$, and we should further investigate the conditions which have to be imposed on the function $f(r, t)$ so that the convergence of the series expansion for $T(r, z, t)$ and $T'(r, z, t)$ is valid. The temperature equations (4.2) and (4.2) can be expressed as

$$T(r, z, t) = \left(\frac{2\kappa Q_0}{\lambda h} \right) \sum_{n=1}^{M'} \frac{1}{C_n} \sum_{l=0}^{M''} \varphi_{nl} S_0(\bar{k}_1, \bar{k}_2, \mu_n r), \tag{6.1}$$

$$T'(r, z, t) = \left(\frac{4\kappa Q_0}{\lambda h^2} \right) \sum_{n=1}^{M'} \frac{1}{C_n} \sum_{m=1}^{M''} \sin\left(\frac{m\pi z}{h}\right) \sum_{l=0}^{M'''} \psi_{nl} S_0(\bar{k}_1, \bar{k}_2, \mu_n r). \tag{6.2}$$

We impose conditions so that both $T(r, z, t)$ and $T'(r, z, t)$ converge in some generalized sense to $g(r, s)$ and $h(r, s)$ respectively as $t \rightarrow 0$ in the transform domain as stated in Section 2. Taking into account the asymptotic behaviour of $\mu_n, S_0(k_1, k_2, \mu_n r)$ and C_n as given in [4], it is observed that the series expansion for both $T(r, z, t)$ and $T'(r, z, t)$ will be convergent by one term approximation as

$$\begin{aligned} \left\{ \begin{matrix} \varphi'_{nl} \\ \psi'_{nl} \end{matrix} \right\} &= \int_0^t \bar{f}(n, t') \left\{ \begin{matrix} \exp[-\kappa(\mu_n^2 + \lambda_l^2)(t-t')] \\ \exp[-\kappa(\mu_n^2 + p^2)(t-t_0)] \end{matrix} \right\} dt' \\ &= O \left\{ 1 / \left(\frac{\mu_n^2 + \lambda_l^2}{\mu_n^2 + p^2} \right)^\kappa \right\}, \quad \text{for } \kappa > 0. \end{aligned} \tag{6.3}$$

Here $\bar{f}(n, t')$ in equation (6.3) can be chosen as one of the following functions or their combination involving addition or multiplication of *constant*, $\sin(\omega t)$, $\cos(\omega t)$, $\exp(kt)$, or *polynomials* in t . Thus, both $T(r, z, t)$ and $T'(r, z, t)$ are convergent to a limit both $\{T(r, z, t), T'(r, z, t)\}_{r=b, z=h}$ as convergence of a series for $r = b$ implies convergence for all $r \leq b$ at any value of z . But for an exact solution would require the use of an infinite number of terms in the equations. In the present solution only the first 10 terms of the transcendental equation $J_p(\alpha, \mu a)Y_p(\beta, \mu b) - J_p(\alpha, \mu b)Y_p(\beta, \mu a) = 0$ and other infinite series are used. The effect of truncating of numbers are brought out by the comparison Table 1 for solutions of different functions for 2, 6 and 10 terms.

It is evident from the table that the convergence is rapid for the temperature distribution for cooling process and axial stress during heating process. The

Functions	2 terms used	6 terms used	10 terms used
$\theta(\xi, \zeta, \tau)$	-0.482	-5.486	-12.091
$\theta'(\xi, \zeta, \tau)$	-24.607	-415.866	-2.601E3
Σ_{rr}	-523.423	-1.028E3	-1.883E3
$\Sigma_{\theta\theta}$	2.585E3	2.072E5	7.535E5

Table 1: Convergence of solution as the number of terms used in the equation are increased from 2 to 10

convergence is somewhat slower in the case of temperature distribution and radial stress for heating processes, it is estimated from table that the possible error from the table is less than 2 percent.

7. Numerical Results, Discussion and Remarks

To interpret the numerical computation we consider material properties of low carbon steel (AISI 1119), which can be used for medium duty shafts, studs, pins, distributor cams, cam shafts, and universal joints having mechanical and thermal properties $\kappa = 13.97 [\mu m/s^2]$, $\nu = 0.29$, $\lambda = 51.9 [W/(m - K)]$, and $a_t = 14.7[\mu m/m - ^\circ C]$. With the general convention that the thickness of a thin annular disc is taken \leq (diameter /40) as $h = 0.04m$, with radius $a = 0.50m$ and $b = 0.85m$ and radiation constant $\bar{k}_1 = \bar{k}_2 = 0.86$.

$$\alpha = \left(\frac{2\kappa Q_0}{\lambda h} \right), \quad \beta = -(1 + \nu)a_t \left(\frac{2\kappa Q_0}{\lambda h} \right), \quad \delta = 2\mu(1 + \nu)a_t \left(\frac{2\kappa Q_0}{\lambda h} \right), \quad (7.1)$$

and further for convenience, we introduce the dimensionless quantities as

$$\begin{aligned} (\xi, \zeta, \bar{a}, \eta) &= \frac{(r, z, a, b)}{a}, \quad (\tau, \tau_0) = \frac{(t, t_0)\kappa}{a^2}, \quad (\Theta, \Theta') = \frac{(T, T')}{\alpha}, \\ \Psi &= \frac{\phi}{\beta}, \quad (\Sigma_{rr}, \Sigma_{\theta\theta}) = \frac{(\sigma)_{rr}, \sigma_{\theta\theta}}{a}. \end{aligned} \quad (7.2)$$

In the foregoing analysis will be illustrated by the numerical results shown in Figure 2 to 7. Figure 2 and 3 depicts the distributions of the dimensionless temperature increment $\theta(\xi, \zeta, \tau)$ and $\theta'(\xi, \zeta, \tau)$ verse dimensionless radius at different values of time with $\zeta = 0.02$. It shows that heat gain on both boundary is zero and then initially temperature increment decreases slowly with increase of radius and the physical meaning emphasis for this phenomenon is that there is reduction in the rate of heat propagation then follows the sinusoidal nature crossing the inner core approaching towards outer edge leading to compressive

radial stress at inner part and expand more on outer due to partially distributed heat supply. The difference in both the results lies with the increasing slope in Figure 3 compared to Figure 2 may be due to the cooling process once the partial heating is removed. Figure 4 depicts the displacement function and it is noteworthy that it is in agreement with the boundary condition (3.7) and attains minimum at the center. Figure 5 and 6 shows the distributions of the radial and axial thermal stresses at different value of time. The stresses Σ_{rr} is smaller than stress $\Sigma_{\theta\theta}$ from Figures 5-6. Figure 7 depicts the distributions of the radial stresses versus dimensionless thickness showing the sinusoidal nature with increasing trend of peak with the fixed value of dimensionless time $\tau = 0.02$. Further in order to investigate the outer radius-to-inner radius ratio $\eta = b/a$ and effects of thickness on the dimensionless temperature distributions and stresses are shown in Figure 8 to 11. Selecting higher outer radius-to-inner radius ratio $\eta = 2.5$ temperature increment and stresses versus dimensionless radius with fixed value of dimensionless thickness $\zeta = 0.02$ attains maximum peak comparative to Figures 2, 3, 5 and 6. Similarly with increase in thickness $\zeta = 0.06$ as shown in Figure 12 temperature radial stress versus dimensionless radius with fixed value of dimensionless thickness $\zeta = 0.02$ attains maximum peak comparative to Figure 7.

8. Conclusion

In this problem, we modify the conceptual ideal proposed by Noda et al (1997) for circular plate. The temperature distributions, displacement and stress functions at the edge $z = h$ occupying the region of the annular disc $a \leq (x^2 + y^2)^{1/2} \leq b$, $0 \leq z \leq h$ have been obtained with the known source function $-(Q_0/\lambda)f(r, t)$. We develop the analysis for the temperature field for both heating and cooling process by introducing the transformation defined by Marchi et al, finite Fourier sine transform and Laplace transform techniques with boundary conditions of radiations type. The series solutions converge provided we take sufficient number of terms in the series. Since the thickness of annular disc is very small, the series solution given here will be definitely convergent. Any particular case can be derived by assigning suitable values to the parameters and functions in the series expressions. The temperature, displacement and thermal stresses that are obtained can be applied to the design of useful structures or machines in engineering applications.

Acknowledgments

Author are thankful to University Grant Commission, New Delhi to provide the partial financial assistance under major research project scheme.

References

- [1] M. Ishihara, Y. Tanigawa, R. Kawamura, N. Noda, Theoretical analysis of thermoelastic-plastic deformation of a circular plate due to a partially distributed heat supply, *Journal of Thermal Stresses*, **20**, No. 2 (1997), 203-233.
- [2] K.W. Khobragade, V. Varghese, N.W. Khobragade, An inverse transient thermoelastic problem of a thin annular disc, *Applied Mathematics E-Notes*, **3** (2006), 617-625.
- [3] N.L. Khobragade, K.C. Deshmukh, Thermoelastic problem of a thin circular plate subjected to a distributed heat supply, *Journal of Thermal Stresses*, **28** (2005), 171-184.
- [4] E. Marchi, G. Zgrablich, Vibration in hollow circular membranes with elastic supports, *Bulletin of the Calcutta Mathematical Society*, **22**, No. 1 (1964), 73-76.
- [5] W. Nowacki, The state of stress in a thick Circular plate due to temperature field, *Bull. Sci. Acad. Polon Sci. Tech.*, **V** (1957), 227.
- [6] S.K. Roy Choudhuri, A note on the quasi-static stress in a thin circular plate due to transient temperature applied along the circumference of a circle over the upper face, *Bull. Acad. Polon. Sci. Ser., Sci. Tech.*, No. 1 (1972), 20-24.
- [7] I.N. Sneddon, *Fourier Transform*, McGraw Hill Book Company (1951).
- [8] P.C. Wankhede, On the quasi-static thermal stresses in a circular plate, *Indian J. Pure and Applied Math.*, **13**, No. 11 (1982), 1273-1277.